Toward a Synthetic Model for Distribution System Restoration and Crew Dispatch

Bo Chen, *Member, IEEE*, Zhigang Ye, *Student Member, IEEE*, Chen Chen, *Member, IEEE*, Jianhui Wang, *Senior Member, IEEE*, Tao Ding, *Member, IEEE*, and Zhaohong Bie, *Senior Member, IEEE*

***Abstract*—Distribution service restoration (DSR) is critical for improving the resilience and reliability of modern distribution systems by strategically and sequentially energizing the system components and customer loads. Restoring electricity service to affected customers also requires multiple crews with different skill sets to perform multiple tasks that are procedurally interdependent with safety guaranteed. However, in existing DSR practices, switch operations and crew dispatch are scheduled separately, and their interdependence is not fully considered. As advanced technologies are enabling remote communication, control, and dispatch, utilities now desire an integrated DSR framework to achieve seamless coordination among multiple DSR tasks such as switch operation, crew dispatch, and component repair. In this paper, we introduce a synthetic model that integrates the service restoration model and the crew dispatch model based on a universal routing model. The proposed model can provide the estimated time of restoration (ETR) for each load, the switching sequence for safely operating remotely/manually operated switches, and dispatch solutions for crews with different skill sets. The proposed synthetic model is formulated as a mixed-integer linear programming (MILP) model, and its effectiveness is evaluated via the IEEE 123 bus test feeder and several large-scale test feeders (EPRI Ckt5, Ckt7, Ckt24 and IEEE 8500 node test feeder).**

***Index Terms*—Distribution service restoration, crew dispatch, mixed-integer linear programming, repair, switching sequence management**

I. INTRODUCTION

Increasingly in recent years, natural disasters are attributed with causing widespread social and economic effects, including large-scale power outages, and they normally take utility companies several weeks before they can completely restore electricity service [1, 2]. Recent hurricanes Nate, Maria, Irma, and Harvey had caused massive customer outages and taken utilities great efforts to restore affected customers, as reported in [3].

The daily power outages of distribution systems, which are caused by randomly occurred short circuit or scheduled component replacement and maintenance, are normally restricted to a local area. In this situation, it is relatively easy to restore the power to the affected customers through system topology reconfiguration to re-route the energization paths by operating the switches installed in the system [4-6]. Meanwhile, repair crews are dispatched to the field to repair the faulted components [7]. It is worth noting that remote-controlled switches can be controlled by the system operator, whereas manually operated switches must be operated by a qualified crew [7, 8]. In the latter case, the crew must travel to the actual switch location, pinpoint the pole where the switch is mounted, and perform a series of procedures to operate the switch safely. Normally, it takes much longer time for crews to repair damaged components and operate (open/close) manual switches. In practice, power utilities use outage management systems (OMS) to handle power outages. The effectiveness of OMS normally depends on its functional modules such as fault location, isolation, and service restoration (FLISR) [9], switching order management [10], crew management [7], call entry and visualization, etc. Existing distribution service restoration (DSR) and crew management are separated applications involving different time scales in OMS. Once an outage is located and isolated, the restoration process will involve two stages: (1) DSR will be triggered first to reconfigure the system topology using remote-controlled switches; (2) the crews will be dispatched to the field to clear fault, repair the damaged components and operate the manually-controlled switches. This kind of restoration scheme is efficient for normal outage scenarios with very few outages, however it is not efficient for restoring large number of outages during extreme events.

In the case of extreme events, such as hurricanes that can cause multiple power outages within a short period of time and

The work of B. Chen, C. Chen, and J. Wang was supported by the U.S. Department of Energy's Solar Energy Technologies Office. The work of T. Ding and Z. Bie was supported by the Science and Technology Project of SGCC (5202011600UG).

B. Chen and C. Chen are with the Energy Systems Division, Argonne National Laboratory, Argonne, IL 60439 USA (e-mail: bo.chen@anl.gov, morningchen@anl.gov).

Z. Ye is with the State Key Laboratory of Electrical Insulation and Power Equipment, Xi'an Jiaotong University, Xi'an, Shaanxi, 710049, China, and the Energy System Division, Argonne National Laboratory, Argonne, IL 60439 USA (e-mail: yzhg.2009@stu.xjtu.edu.cn, zhigang.ye@anl.gov).

J. Wang is with the Department of Electrical Engineering at Southern Methodist University, Dallas, TX, USA (email: jianhui@mail.smu.edu).

T. Ding and Z. Bie are with Xi'an Jiaotong University, Xi'an, Shaanxi, 710049, China (email: tding15@mail.xjtu.edu.cn, zhbie@mail.xjtu.edu.cn).

leave a large region within utility service territories without power, not all remote-controlled switches are available and safe to operate. In this case, repair crews must clean and repair the components that prevent the remote-controlled switches from operating. For example, the repair crew need to fix the upstream faulty lines such that the downstream remote-controlled switches can be operated. Meanwhile, the repair work must be performed in a safe condition, which sometimes requires to lock the upstream remote-controlled switch. In this sense, crew dispatch and switching order management are tightly coupled and become an operational challenge facing system operators. Therefore, seamless coordination among DSR and crew dispatch is the key to enhancing restoration efficiency and to effectively reducing outage minutes. While the performance of each OMS module is critical for reducing the outage duration, it is equally important to improve the interoperability of different OMS modules to further minimize the outage impact.

In the context of active distribution system (ADS), an optimal DSR solution should contain a sequence of temporally interdependent control actions [11, 12] that can coordinate various controllable components over a time horizon, such as distributed generators (DGs) [13, 14], microgrids [15-18] and remote-controlled switches [19, 20]. In the recent works which considers the sequence of abovementioned controllable components [4, 5, 21-24], the time horizon is pre-determined and divided into multiple fixed-length time steps (for simplicity, we refer them as fixed-time step (FTS) models). In practice, the time for crews to perform operation and repair tasks is usually much longer than the time for dispatching and operating DGs and switches. Therefore, FTS models are facing two trade-offs between computational performance and solution optimality to integrate both DSR and crew dispatch problems: (1) the dilemma for choosing time horizon: longer horizon captures more information of the repair and restoration process but involves more variables to define and hence the computation burden will be increased, while shorter horizon saves computation time but cannot guarantee scheduling all the repair tasks; (2) the dilemma for choosing the length of time intervals: longer interval results in inaccurate solutions but relieves computation burden, while shorter interval is more accurate but increases the computation time. The research on DSR and crew dispatch integration is still at early stage in recent years with many concerns unaddressed. A. Arab and Z. Han et al.[25] proposed a mixed-integer linear programming (MILP) model to assign repair crews to damaged components while ignoring the travel time and routing sequence. P. Van Hentenryck and C. Coffrin et al. [26-28] decoupled power restoration and crew routing problems to improve the computation efficiency at the cost of compromising the solution optimality. A. Arif and Z. Wang et al. [29, 30] formulated the problem using a fix-time step model and applied heuristic techniques. The results demonstrated the advantages of integrating DSR and crew repair problems over traditional methods. To the best of our knowledge, the existing methods did not consider the switch operation performed by crews, which is a critical operation during DSR. Furthermore, the computational capability required for solving the integrated model appears to be a major concern.

To overcome the aforementioned challenges, this paper introduces a synthetic model for DSR and crew dispatch based on a synthetic routing model. The proposed model bypasses the dilemma of selecting the time intervals and can be easily extended to consider various procedural constraints. The proposed synthetic model can be also extended to consider crews with other skill sets, such as resource transportation and vegetation management. The remainder of this paper is organized as follows. Section II describes integrated DSR and crew dispatch. Section III introduces the universal routing model. Section IV introduces the mathematical synthetic model. Section V provides numerical results to validate the proposed synthetic model. Conclusions and future work are discussed in Section VI.

II. Integrated DSR and Crew Dispatch

In conventional OMS, the DSR module and crew dispatch module function separately with limited coordination. When facing large-scale power outages caused by extreme weather events, system operators find it difficult to determine the optimal restoration plan that can specify the switching sequence for switches and assign detailed task orders for every crewmember. If crews are not properly dispatched to perform the designated tasks, system operators must revise the restoration plan accordingly. Therefore, an integrated model that can achieve seamless coordination between DSR and crew dispatch will be preferred by the system operators.

A. Integrated Framework

To achieve the seamless integration of DSR and crew dispatch, an integrated framework should be developed, where the integration is implemented mainly through four stages, as shown in Fig. 1. In Stage 1, various sources of data are collected from the supervisory control and data acquisition (SCADA) system, the customer information system (CIS), the smart meter, field crew report, and distribution management system (DMS). In Stage 2, the data collected enable the OMS to perform data fusion and visualization, locate and isolate the faulted areas, assess the faulted components, and perform initial-stage restoration. The field crews dispatched for damage assessment will report the damage status, initiate a repair request, and estimate the repair time. In the initial-stage restoration, the switches will be operated strategically to isolate and minimize the faulted areas. It is worth noting that the initial-stage restoration involves only “healthy” and remote-controlled switches that are not affected by the severe weather conditions. The optimal switching model for the initial-stage restoration is outside the scope of this paper. Next, the system operator will dispatch field crews to open manually operated switches to further isolate the faulted areas. Eventually, the system operator in OMS will be updated with the most current system states, including the damage status of system components, estimated repair time, current status of all of the switches, and the number of affected customers, etc. With all of this information available,

the integrated DSR and crew dispatch engine developed in Stage 3 will generate the restoration solution accordingly. In this paper, we assume the crews can be categorized into two groups: (1) crew for operation, and (2) crew for repair. The crew for operation is responsible for operating the manually operated switches; and the crew for repair is responsible for repairing any faulted components including switches. We assume that the crew for repair is also capable of operating the manually operated switches under de-energized condition right after the repair is done. In Stage 4, the restoration plan will be executed by sequentially operating the remote-controlled switches and assigning task orders to crews. The system state will be updated accordingly. The integrated DSR and crew dispatch engine will continuously generate updated solutions in response to unexpected events, such as succeeding outages, unfinished task orders, and switch malfunction.

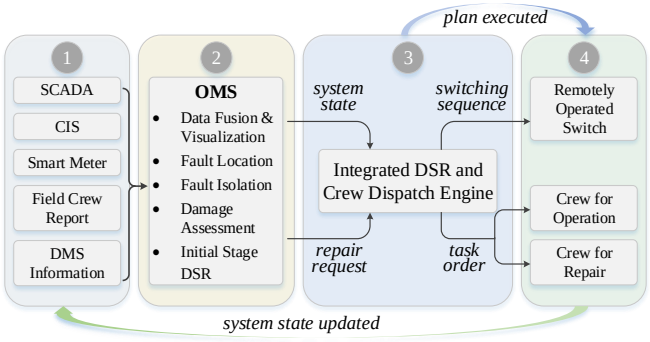

Fig. 1. The integrated framework for DSR and crew dispatch.

B. Interdependence between DSR and Crew Dispatch

In OMS, both the DSR and crew dispatch modules are serving the objective of minimizing the affected customers and restoring the electricity service as quickly as possible. To achieve this objective, the interdependence between the domains (i.e., DSR, crew for operation, and crew for repair) must be identified, as summarized in TABLE I. To illustrate the interdependency, Fig. 2 shows the system diagram of a simple distribution feeder. The feeder is subjected to multiple faults on remote switch A2, manual switch M2, line L1, and customer C1. All of the switches are opened to isolate the faulted components. For safety reasons, the switches used for isolating a particular faulted component are locked until the repair is completed. To restore the system, the remote switches should be closed sequentially, and crews should be dispatched to repair the faulted components and operate the manual switches in a strategically scheduled order. Fig. 3 shows an example restoration solution, where the solution involves several entities: the service restoration program (DSR), one crew for operation (Crew 1), and two crews for repair (Crews 2 and 3). To operate a remote/manual switch, the lock status, if any, must be removed by repairing the associated components. For example, Crew 2 is dispatched to repair L1 isolated by A1 and M1. Both A1 and M1 should be kept open as Crew 2 is in the process of repair. Once L1 is repaired, the lock on A1 is removed and A1 is closed to energize a small segment of the feeder. However, M1 still remains locked in order to isolate faulted M2. As Crew 3 travels to M2 and finishes the repair, both M1 and M2 will be unlocked. After a short period of time, Crew 1, which leaves the depot at the same time as Crews 2 and 3, arrives at and closes M1. Then, Crew 1 travels to and closes M2, after confirming that the repair work is done by the repair crew. Similarly, A2 is closed after being repaired by Crew 2.

TABLE I. INTERDEPENDENCE BETWEEN DSR AND CREW DISPATCH

Domain			Interdependence Description
DSR	*Crew for Operation*	*Crew for Repair*	
√	√		A crew operates a manually operated switch to energize components.
	√	√	A switch can be operated only after the lock status, if any, is removed.
√		√	A faulted component can be energized only after being repaired. The crew can operate the switch right after the repair.
√	√	√	To repair a faulted component, the component should be isolated by opening upstream/downstream switches to ensure crew safety. A switch cannot be energized when an operation crew is in the process of operating it.

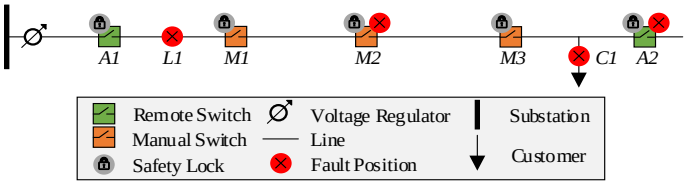

Fig. 2. An example system subjected to multiple faults.

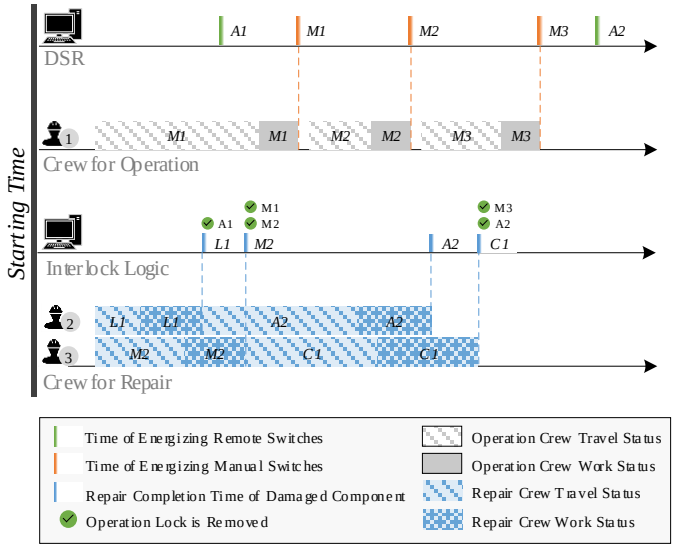

Fig. 3. An example solution considering the interdependence between DSR and crew dispatch.

The example indicates that optimal coordination between the DSR and crew dispatch requires the full consideration of the travel time, repair time, operation time, and interdependence. The power system constraints, such as thermal limits and voltage profiles, further complicate the problem. As real-life systems normally contain multiple feeders, crews, and depots,

realizing optimal coordination becomes very difficult for system operators by relying on their own experience. To address these issues and challenges, we propose a synthetic mathematical model for DSR and crew dispatch based on a universal routing model introduced in the following sections.

III. Universal Routing Model

The crew dispatch problem can be inherently formulated as a classic routing model by modeling each crew as a travel agent. In contrast, the DSR problem is normally formulated as a multiple-step dynamic optimization model, where the time interval between any two consecutive steps is fixed, thereby causing inefficient integration with routing models because of the heterogeneity between the two models. In this section, we propose a universal routing model by formulating the DSR problem as a routing problem and interdependence as a set of constraints.

A. Energization Agent and Energization Path

Considering the process of DSR, the electricity travels along the feeders from the sources (e.g., substations) to energize downstream customers. The switching sequences for the switches determine the energization paths, that is, the routes along which the electricity should travel. For distribution systems operated in radial topology, multiple energization paths may be established to connect the sources and the customers without forming loops. In this sense, the DSR problem can be formulated as a routing problem by assuming each energization sequence to be an energization path, and an energization agent travels along the energization path. The difference between the aforementioned model and the traditional routing model is that, instead of assigning a fixed number of travel agents in advance, the energization agent can "split" into multiple energization agents when multiple downstream lines need to be energized. The detailed introduction of the concept of an energization agent can be found in the authors' previous work [31].

B. Node Cell

Node cell is defined as a group of system components interconnected by non-switchable lines [24]. Multiple node cells are interconnected through switches. All the components within a node cell can be energized at once by closing any one of the switches connected to it.

C. Route Table and Arrival Time Table

The route table and arrival time table, which are commonly used concepts in routing problems, can be used to formulate the activities of different entities in the context of the proposed synthetic model. We assume that there are three types of travel agents: the operation agent (OA), repair agent (RA), and energization agent (EA). For each type of agent, we can model its activity using a graph $G(\mathcal{N},\mathcal{E})$ with $\mathcal{N}$ as the set of nodes that the agent may visit, and $\mathcal{E}$ as the set of paths that the agent may travel. As shown in Fig. 4 (a), $\mathcal{N}$ represents the depots and manual switches for OA, the depots and faulted components for RA, and the substations and node cells for EA.

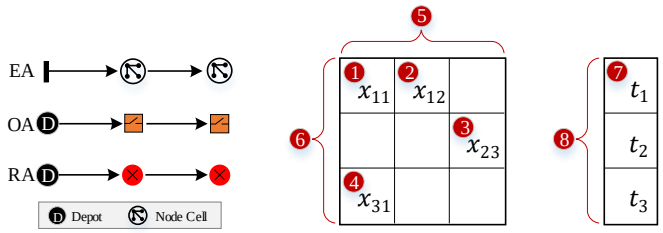

(a) (b) (c)

Fig. 4. The concepts of route table and arrival time table in the routing problem: (a) three types of travel agents, (b) route table, and (c) arrival time table.

For each type of agent, the interpretation of the entries in the route table and arrival time table is marked in Fig. 4 (b–c), and explained in TABLE II. Various procedural interdependencies can be formulated as constraints of the entries in both tables.

TABLE II. Definition of Variables in Route and Arrival Time Tables

No.	Variable	Definition
①	x_{ii}	*Diagonal terms of the route table.* $x_{ii}=1$, if node i is the substation for EA or the depot for OA and RA. It is also the "starting point" for associated agents. $x_{ii}=0$, if node i is not the "starting point."
②③④	$x_{ij}, i\neq j$	*Off-diagonal terms of the route table.* $x_{ij}=1$, if the agent travels from node i to node j. Otherwise, $x_{ij}=0$. $x_{ij}=x_{jk}=1$ indicates that the agent travels by following the sequence $i\rightarrow j\rightarrow k$.
⑤⑥	-	*Dimension of the route table.* The route table is an $n\times n$ matrix, where n is the number of node cells for EA, the number of manual switches and depots for OA, and the number of faulted components and depots for RA.
⑦	t_i	*Entry of the arrival time table.* t_i represents the arrival time when an agent arrives at node i. If $x_{ij}=1$, t_j-t_i is the travel time.
⑧	-	*Dimension of the arrival time table.* The arrival time table is an $n\times 1$ matrix, where n is the same as the dimension of the route table.

IV. Mathematical Model

A. Notation

We use superscripts 'E', 'O,' and 'R' to denote the variables that are associated with EA, OA, and RA, respectively. The notations in this section are listed in TABLE III.

B. Routing Model Constraints for OA, RA, and EA

As mentioned in Section III, the universal routing model can be applied when formulating OA, RA, and EA routing problems. Route table constraints for OA, RA, and EA routing problems are specifically summarized in TABLE IV. Each type of agent has a set of similar constraints that regulate its traveling activities. Note that for EA, constraints (9), (18), and (19) ensure that the EA agents travel through the networks without forming loops, thus guaranteeing a radial topology.

TABLE III. NOTATIONS OF THE MATHEMATICAL MODEL

Indices and Sets	
$\mathcal{D}^O, \mathcal{D}^R$	Set of depots for OA/RA
$\mathcal{SW}^E, \mathcal{M}^O, \mathcal{A}^E$	Set of all/manual/remote switches
$\mathcal{G}^E, \mathcal{G}_f^E$	Set of all/faulted power source cells
$\mathcal{B}^E, \mathcal{B}_f^E$	Set of all/faulted branches
$\mathcal{L}^E, \mathcal{L}_f^E$	Set of all/faulted critical loads
$\mathcal{F}^R$	Set of all faulted components
$\mathcal{C}^E$	Set of node cells
$e^r(i,j)$	Index transfer from EA to RA for switch (i,j)
$e^o(i,j)$	Index transfer from EA to OA for switch (i,j)
$r^e(i)$	Index transfer from RA to EA for faulted component i
$l^c(i)$	Index transfer from load c to its cell for load i
Parameters	
n^O, n^R, n^E	Number of operation sites, repair sites, and electric cells
$n_{cap,i}^O, n_{cap,i}^R$	Number of operation/repair crews in depot i
T_{ii}^O, T_{ii}^R	Start time for operation/repair routing
T_{ij}^O, T_{ij}^R	Travel time between two operation/repair sites
T_{rs}^E, T_{ms}^O	Operation time for remote/manual switch
T_i^{RP}	Repair time for faulted component i
T^{MAX}	Time limit for OA to operate manual switches
β_i^L	Weight for load i
M	A large positive number
Variables	
$x_{ij}^O, x_{ij}^R, x_{ij}^E$	Route table elements for OA/RA/EA
t_i^O, t_i^R, t_i^E	Arrival time table elements for OA/RA/EA
f_j^R	Restoration completion time when all the damages inside node cell j are repaired
$d_{ij}^{MS_O}, d_{ij}^{MS_R}$	Binary variable indicating whether OA/RA will operate manual switch
$d_{ij}^{MS_e}, d_{ij}^{MS_{de}}$	Binary variable indicating whether OA will operate energized/de-energized manual switch
$s_{i,t_p}^E, x_{ij,t_p}^B$	Energization status for node i/branch (i,j) at time t_p

$$t_i^O \geq T^{MAX} - M\sum_{h=1,h\neq i}^{n^O} x_{hi}^O \\ t_i^O \leq T^{MAX} + M\sum_{h=1,h\neq i}^{n^O} x_{hi}^O \Big\}, \forall i \in \mathcal{M}^O. \quad (23)$$

$$t_i^R = T_{ii}^R,\ \forall i \in \mathcal{D}^R. \quad (24)$$

$$t_j^R \geq t_i^R + T_{ij}^R - \left(1 - x_{ij}^R\right)M \\ t_j^R \leq t_i^R + T_{ij}^R + \left(1 - x_{ij}^R\right)M \Big\}, \forall i \in \mathcal{D}^R, \forall j \in \mathcal{F}^R. \quad (25)$$

$$t_j^R \geq t_i^R + T_{ij}^R + T_i^{RP} - \left(1 - x_{ij}^R\right)M \\ t_j^R \leq t_i^R + T_{ij}^R + T_i^{RP} + \left(1 - x_{ij}^R\right)M \Big\}, \\ \forall i \in \mathcal{F}^R \backslash \mathcal{M}^O, \forall j \in \mathcal{F}^R, i \neq j. \quad (26)$$

$$t_j^R \geq t_i^R + T_{ij}^R + T_i^{RP} + T_{ms}^O d_{r^e(i)}^{MS_R} - \left(1 - x_{ij}^R\right)M \\ t_j^R \leq t_i^R + T_{ij}^R + T_i^{RP} + T_{ms}^O d_{r^e(i)}^{MS_R} + \left(1 - x_{ij}^R\right)M \Big\}, \\ \forall i \in \mathcal{F}^R \cap \mathcal{M}^O, \forall j \in \mathcal{F}^R, i \neq j. \quad (27)$$

$$t_i^R \geq T^{MAX} - M\sum_{h=1,h\neq i}^{n^R} x_{hi}^R \\ t_i^R \leq T^{MAX} + M\sum_{h=1,h\neq i}^{n^R} x_{hi}^R \Big\}, \forall i \in \mathcal{F}^R \quad (28)$$

$$t_i^E = T_{ii}^E, \forall i \in \mathcal{G}^E \backslash \mathcal{G}_f^E. \quad (29)$$

$$t_j^E \geq \max(t_i^E, f_j^R) + T_{rs}^E - \left(1 - x_{ij}^E\right)M \\ t_j^E \leq \max(t_i^E, f_j^R) + T_{rs}^E + \left(1 - x_{ij}^E\right)M \Big\}, \\ \forall (i,j) \in \mathcal{A}^E \backslash \mathcal{B}_f^E. \quad (30)$$

$$f_{r^e(i)}^R \geq t_i^R + T_i^{RP}, \forall i \in \mathcal{F}^R. \quad (31)$$

$$f_j^R = 0, \forall\, j \in \mathcal{C}^E, j \cap r^e(\mathcal{F}^R) = \emptyset. \quad (32)$$

$$t_i^E \geq T^{MAX} - M\sum_{h=1,h\neq i}^{n^E} x_{hi}^E \\ t_i^E \leq T^{MAX} + M\sum_{h=1,h\neq i}^{n^E} x_{hi}^E \Big\}, \forall i \in \mathcal{C}^E \backslash \mathcal{G}^E \quad (33)$$

The independent arrival time constraints for OA, RA, and EA can be formulated as constraints (20–23), (24–28), and (29–33), respectively. Constraint (20) defines the initial time when an OA starts traveling. Constraint (21) requires that the to-site arrival time of an OA should not be less than the from-site arrival time plus the travel time if an OA leaves from depot i to a manual switch j. The additional manual switch operation time is considered in (22) if an OA travels from manual switch i to another manual switch j. Constraint (23) sets the close time to be a large value T^{MAX} if a manual switch is not visited by an OA throughout the restoration process. In this paper, we set T^{MAX} to be 1,440 min. (i.e., one day). Constraint (24) defines

TABLE IV. ROUTE TABLE CONSTRAINTS FOR OA, RA, AND EA ROUTING PROBLEMS

Route Table Constraints	**Travel Agents Defined in the Universal Routing Model**		
	OA	*RA*	*EA*
Each type of agent should travel starting only from the depot/substation.	$x_{ii}^O = 1, \forall i \in \mathcal{D}^O$ (1) $x_{ii}^O = 0, \forall i \in \mathcal{M}^O$ (2)	$x_{ii}^R = 1, \forall i \in \mathcal{D}^R$ (3) $x_{ii}^R = 0, \forall i \in \mathcal{F}^R$ (4)	$x_{ii}^E = 1, \forall i \in \mathcal{G}^E$ (5) $x_{ii}^E = 0, \forall i \in \mathcal{C}^E \backslash \mathcal{G}^E$ (6)
Each type of agent should not go back to the depot/substation. An EA can travel from one cell to another cell only along existing switches.	$x_{ij}^O = 0, \forall i,j \in \mathcal{D}^O, i \neq j$ (7)	$x_{ij}^R = 0, \forall i,j \in \mathcal{D}^R, i \neq j$ (8)	$\sum_{h=1,h\neq i}^{n^E} x_{hi}^E = 0, \forall i \in \mathcal{G}^E$ (9) $x_{ij}^E = x_{ji}^E = 0, \forall (i,j) \notin \mathcal{B}^E$ (10)
Each possible route can be visited no more than once.	$x_{ij}^O + x_{ji}^O \leq 1, \forall i,j \in \mathcal{D}^O \cup \mathcal{M}^O$ (11)	$x_{ij}^R + x_{ji}^R \leq 1, \forall i,j \in \mathcal{D}^R \cup \mathcal{F}^R$ (12)	$x_{ij}^E + x_{ji}^E \leq 1,\ \forall (i,j) \in \mathcal{B}^E$ (13)
The total number of agents dispatched out of each OA or EA depot cannot exceed the capacity of that depot.	$\sum_{j=1,j\neq i}^{n^O} x_{ij}^O \leq n_{cap,i}^O,\ \forall i \in \mathcal{D}^O$ (14)	$\sum_{j=1,j\neq i}^{n^R} x_{ij}^R \leq n_{cap,i}^R,\ \forall i \in \mathcal{D}^R$ (15)	–
For each type of agent, each destination can be visited by at most one agent. For OA and RA, an agent should leave or stay at the visited destination. For EA, an agent leaving a visited destination can split into multiple agents.	$\sum_{j=1}^{n^O} x_{ij}^O \leq \sum_{h=1}^{n^O} x_{hi}^O \leq 1, \forall i \in \mathcal{M}^O$ (16)	$\sum_{j=1}^{n^R} x_{ij}^R \leq \sum_{h=1}^{n^R} x_{hi}^R \leq 1, \forall i \in \mathcal{F}^R$ (17)	$\sum_{h=1}^{n^E} x_{hi}^E \leq 1, \forall i \in \mathcal{C}^E$ (18) $\sum_{j=1}^{n^E} x_{ij}^E \leq n^E \sum_{h=1}^{n^E} x_{hi}^E, \forall i \in \mathcal{C}^E$ (19)

C. Arrival Time Table Constraints

1) Independent Constraints

$$t_i^O = T_{ii}^O,\ \forall i \in \mathcal{D}^O. \quad (20)$$

$$t_j^O \geq t_i^O + T_{ij}^O - \left(1 - x_{ij}^O\right)M, \forall i \in \mathcal{D}^O, \forall j \in \mathcal{M}^O. \quad (21)$$

$$t_j^O \geq t_i^O + T_{ij}^O + T_{ms}^O - \left(1 - x_{ij}^O\right)M, \forall i,j \in \mathcal{M}^O, i \neq j. \quad (22)$$

the initial time when an RA starts traveling. Constraints (25–27) limit the to-site *j* arrival time of an RA, which should be equal to from-site arrival time *i* plus travel time, travel repair time, travel repair and manual switch operation time, respectively, for the case that from-site *i* is depot, faulted component (not manual switch), and faulted manual switch, respectively. It should be noted that $d_{r^e(i)}^{MS_R}$ is a binary variable indicating whether a faulted manual switch is switched-on by an RA, and this binary variable will be introduced later in (34–35). Constraint (28) sets the repair time to be T^{MAX} if a faulted component is not repaired by an RA. Constraint (29) defines the initial energized time for healthy substation or black-start DG node. Constraint (30) requires that if an EA travels from *i* to *j* through electric route (i,j), the energization time of node cell *j* (i.e., t_j^R) should depend on both the energization time of *i* and the damage status of *j*, as well as the operation time of the remote-controlled switch between *i* and *j*. If *j* contains damaged components inside, then the cell *j* can only be energized after being repaired. This constraint ensures that before the to-cell *j* is energized, the from-cell *i* must be energized and all the damages inside the to-cell *j* must be repaired. Constraint (31) ensures the repair completion time of cell *j* should be larger than the sum of the arrival time of repair crew and the repair time for every damage insider cell *j*. Constraint (32) ensures that for those node cells without damages, the repair completion time is set to be zero. Constraint (33) sets the energization time of cell *i* to be T^{MAX} if it is not traveled by any other EA.

It is worth noticing that the proposed model assumes that OAs can only operate manual switches, and RAs can only operate a manual switch right after repairing it. However, the model can be further extended to model crews with capabilities of both operating intact manual switches and repairing damaged switches, by setting the intact manual switches as damaged components with required repair time to be zero.

2) Interdependent Constraints

In this section, the arrival time coordination constraints between OA, RA, and EA are formulated.

First, we assume that the switch-on task for manual switch (i,j) can be allocated to either an OA or an RA. The allocation can be indicated using two binary variables, $d_{ij}^{MS_O}$ and $d_{ij}^{MS_R}$, respectively. The task allocation constraints are formulated as:

$$\left.\begin{aligned} d_{ij}^{MS_O} &= 1 \\ d_{ij}^{MS_R} &= 0 \end{aligned}\right\}, \forall e^o(i,j) \in \mathcal{M}^O \backslash \mathcal{F}^R. \quad (34)$$

$$\left.\begin{aligned} d_{ij}^{MS_O} + d_{ij}^{MS_R} &= 1 \\ d_{ij}^{MS_O} &\geq \sum_{h=1}^{n^O} x_{h \cdot e^o(i,j)}^O \\ d_{ij}^{MS_R} &\leq \sum_{h=1}^{n^R} x_{h \cdot e^r(i,j)}^R \end{aligned}\right\}, \forall e^o(i,j), e^r(i,j) \in \mathcal{M}^O \cap \mathcal{F}^R. \quad (35)$$

$$t_{e^o(i,j)}^O \geq t_{e^r(i,j)}^R + T_{e^r(i,j)}^{RP} - (1 - d_{ij}^{MS_O})\, M. \quad (36)$$

Constraint (34) represents that a healthy manual switch can be visited by an OA only. Constraint (35) requires that a faulted manual switch could be visited by either an OA or an RA. When an operation crew visits it, we have $d_{ij}^{MS_O} = 1, d_{ij}^{MS_R} = 0$, which means an OA is responsible for operating the manual switch, if needed. Otherwise, the RA will be responsible for operating this switch, if needed. Constraint (36) ensures that if an OA is to operate the faulted manual switch, the operation time must be at least later than its repair completion time.

Second, the interdependent arrival time constraints between RA and EA are formulated as:

$$t_i^E \geq t_{e^r(i,j)}^R + T_{e^r(i,j)}^{RP} + T_{ms}^O - \left(1 - d_{ij}^{MS_R}\right)M, \quad \forall e^r(i,j) \in \mathcal{M}^O \cap \mathcal{F}^R. \quad (37)$$

$$\left.\begin{aligned} t_j^E &\geq t_i^E - \left(2 - x_{ij}^E - d_{ij}^{MS_R}\right)M \\ t_j^E &\leq t_i^E + \left(2 - x_{ij}^E - d_{ij}^{MS_R}\right)M \end{aligned}\right\}, \forall e^r(i,j) \in \mathcal{M}^O \cap \mathcal{F}^R. \quad (38)$$

$$t_{r^e(i)}^E = t_i^R + T_i^{RP}, \forall i \in \mathcal{G}_f^E. \quad (39)$$

$$t_{r^e(i)}^E \geq t_i^R + T_i^{RP}, \forall i \in \mathcal{B}_f^E \cup \mathcal{L}_f^E. \quad (40)$$

$$\left.\begin{aligned} t_i^E &\geq t_{e^r(i,j)}^R + T_{e^r(i,j)}^{RP} \\ t_j^E &\geq t_{e^r(i,j)}^R + T_{e^r(i,j)}^{RP} \end{aligned}\right\}, \forall e^r(i,j) \in \mathcal{SW}^E \cap \mathcal{F}^R. \quad (41)$$

Constraints (37–38) depict that if an RA is to operate the faulted manual switch, cell *i* must be de-energized before finishing the operation, and cells *i* and *j* must be energized together. Constraint (39) implies that a faulted black-start DG will start immediately after being repaired. Constraint (40) ensures that a cell can only be energized when an RA repairs all faulted lines and critical loads inside the cell. Constraint (41) ensures that both end-cells of a switch (auto and manual) should be de-energized when it is being repaired.

Third, the interdependent arrival time constraints between OA and EA are formulated as:

$$\frac{t_{e^o(i,j)}^O - t_i^E}{M} \leq d_{ij}^{MS_e} \leq \frac{t_{e^o(i,j)}^O - t_i^E}{M} + 1, \forall e^o(i,j) \in \mathcal{M}^O. \quad (42)$$

$$\left.\begin{aligned} t_j^E &\geq t_{e^o(i,j)}^O + T_{ms}^O - \left(3 - x_{ij}^E - d_{ij}^{MS_O} - d_{ij}^{MS_e}\right)M \\ t_j^E &\leq t_{e^o(i,j)}^O + T_{ms}^O + \left(3 - x_{ij}^E - d_{ij}^{MS_O} - d_{ij}^{MS_e}\right)M \end{aligned}\right\}, \quad \forall e^o(i,j) \in \mathcal{M}^O. \quad (43)$$

$$\frac{t_i^E - \left(t_{e^o(i,j)}^O + T_{ms}^O\right)}{M} \leq d_{ij}^{MS_{de}} \leq \frac{t_i^E - \left(t_{e^o(i,j)}^O + T_{ms}^O\right)}{M} + 1, \quad \forall e^o(i,j) \in \mathcal{M}^O. \quad (44)$$

$$\left.\begin{aligned} t_j^E &\geq t_i^E - \left(3 - x_{ij}^E - d_{ij}^{MS_O} - d_{ij}^{MS_{de}}\right)M \\ t_j^E &\leq t_i^E + \left(3 - x_{ij}^E - d_{ij}^{MS_O} - d_{ij}^{MS_{de}}\right)M \end{aligned}\right\}, \quad \forall e^o(i,j) \in \mathcal{M}^O. \quad (45)$$

$$\left.\begin{aligned} d_{ij}^{MS_e} + d_{ij}^{MS_{de}} &\geq 1 - \left(2 - x_{ij}^E - d_{ij}^{MS_O}\right)M \\ d_{ij}^{MS_e} + d_{ij}^{MS_{de}} &\leq 1 + \left(2 - x_{ij}^E - d_{ij}^{MS_O}\right)M \end{aligned}\right\}, \quad \forall e^o(i,j) \in \mathcal{M}^O. \quad (46)$$

Constraints (42–46) imply when OA operates the switch ($d_{ij}^{MS_O} = 1$), it should be ensured that either the cell *i* is energized before OA arrives ($d_{ij}^{MS_e} = 1$), or the cell is de-energized until the OA finishes the operation ($d_{ij}^{MS_{de}} = 1$), which is defined by comparing the time relationship in (42) and (44). Constraint (43) shows that if cell *i* is pre-energized, then cell *j* will be energized after OA finishes the operation, whereas (45) depicts that if cell *i* is de-energized, then cells *i* and *j* will be energized together in later time. Constraint (46) ensures that

cell i cannot be energized during the de-energized operation, which is necessary for the consideration of safety.

Moreover, if manual switch (i,j) cannot be energized, the operation crew should be prevented from closing that switch, which is formulated as:

$$\sum_{h=1}^{n^O} x^O_{h\cdot e^O(i,j)} \le x^E_{ij} + x^E_{ji}, \forall e^O(i,j) \in \mathcal{M}^O. \quad (47)$$

D. Physical System Constraints

Rather than adopting the fixed multi-step model, we use the concept of a checkpoint to reduce the computation burden by considering the operation characteristics of a radially operated distribution system.

A checkpoint is a time instance when we want to check operational constraints. In a radially operated distribution system, when restoring an additional load, the voltage profiles and line loading conditions are monotonically changed along feeders under the assumption that the system is three-phase balanced [32]. In this paper, we assume that all of the currents are unidirectional, that is, flowing from substation to loads. We also assume the loads in each cell are nearly three-phase balanced because of a good switch placement strategy in the planning stage. Thus, restoring an additional cell will lower the entire voltage profile and increase the loading of upstream lines as compared to the system configuration before this load is restored. Obviously, only one instance should be checked when no more loads are restored (denoted by t_p), because the overall voltage profile is normally at the lowest level in this condition. The computational burden thus will be greatly reduced by checking only the operational constraints at t_p, rather than checking numerous time steps in the multi-step time horizon model. The relationship between energization status and route tables is formulated as:

$$s^E_{i,t_p} = \sum_h^{n^E} x^E_{hi}, \forall i \in \mathcal{C}^E. \quad (48)$$

$$x^B_{ij,t_p} = \left(x^E_{ij} + x^E_{ji}\right) s^C_{i,t_p} s^C_{j,t_p}, \forall i,j \in \mathcal{C}^E, (i,j) \in \mathcal{SW}^E. \quad (49)$$

Constraint (48) implies that the energization status of each node cell i at time t_p depends on whether this cell is visited by an EA. Constraint (49) shows that the energization status of switch (i,j) depends on whether this switch is visited by an EA and whether the node cells on both ends are energized at t_p. Because $x^E_{ij} + x^E_{ji}$ is in fact binary because of constraint (13), (49) is the product of three binary variables, which can be linearized with the method in [33].

Other electrical system constraints, which include the linear three-phase power flow model, branch capacity constraints, nodal voltage limit, and component connectivity constraints, as well as topology constraints, can be accessed in the authors' previous work [24].

E. Objective Function

The objective is to minimize the unserved energy, which is formulated as:

$$\min \sum_{i\in\mathcal{L}} \sum_{\phi\in\{a,b,c\}} \beta^L_i P^\phi_i t^E_{l^c(i)} \quad (50)$$

where $t^E_{l^c(i)}$ is the EA arrival time for node cell $l^c(i)$ where load i is located in; ϕ and $\{a, b, c\}$ are index and set of phases, respectively; and P^ϕ_i is the active power demand of load i phase ϕ.

V. Numerical Results

In this section, we validate the proposed synthetic mixed-integer linear programming (MILP) model for DSR and crew dispatch, which are solved by CPLEX 12.8 on an Intel Xeon X5670 (with a 2.93-GHz CPU, 12 GB of RAM, and 64-bit operating system).

A. Test on IEEE 123 Bus Test Feeder

1) Test Feeder and Case Design

Fig. 5 shows the modified IEEE 123 bus test feeder [34, 35], which is a medium size unbalanced distribution system operated at a nominal voltage of 4.16 kV with 3-phase unbalanced loads of total 3385 kW. We modified it by adding five additional switches (i.e., 1-7, 13-18, 23-25, 76-77, 87-89) to form more node cells, while the unbalanced lines, unbalanced loads, regulators and transformers are remained original. As shown in Fig.5, the system is separated into 15 node cells by all the 16 switches. We have performed case studies in two scenarios on this test feeder. We set the MIP gap tolerance to be 1% and time limit to be 3600 seconds in the CPLEX solver.

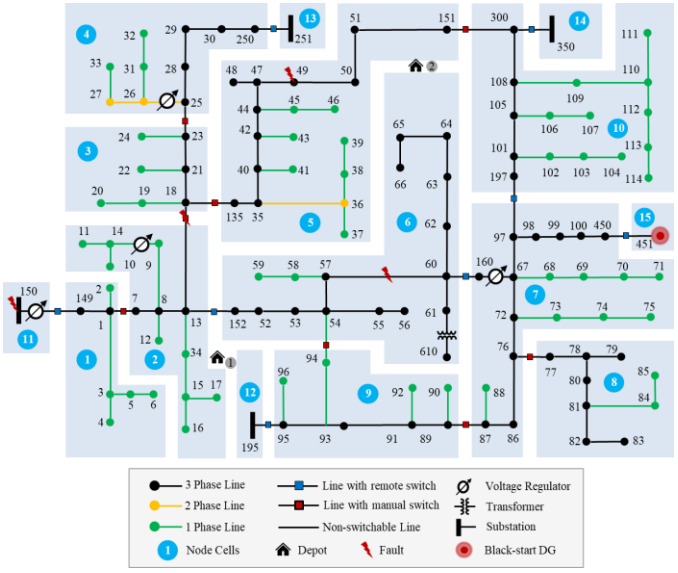

Fig. 5. Modified IEEE 123 node test feeder.

a) Cases for Scenario I

In scenario 1, we assume the system contains 8 remote-controlled switches and 8 manually operated switches. The types and operating time for all switches are listed in TABLE V. We also assume there is a black-start DG placed at node 451, which can be utilized for quick service restoration. The parameters of this DG are listed in TABLE VI. To observe damages for different types of components, we assume four damages which is substation, switch, line and critical load respectively, and the positions and repair time of each damage are listed in TABLE VII. The crews depart from two depots, as shown in Fig. 5, and we assume that crew travelling time between two sites is proportional to their geographic distance, of which the maximum travel time between two sites along this

test feeder is 34 minutes from node 33 to node 83. It should be noted that the selection of all the parameters (switch operating time, component repair time, travel time, etc.) is independent of the proposed model and can be replaced by real data input by operators.

TABLE V. SWITCH OPERATING TIME

Switches	Type	Operating Time (min.)
13-152, 60-160, 97-197, 150-149, 250-251, 450-451, 300-350, 95-195	Remote	1
1-7, 13-18, 23-25, 76-77, 87-89, 18-135, 54-94, 151-300	Manual	15

TABLE VI. DG PARAMETERS

Name	Node	P_g^{max}/P_g^{min} (kW)	Q_g^{max}/Q_g^{min} (kVar)
DG451	451	2,000/0	1,600/−1,000

TABLE VII. DAMAGED COMPONENTS AND REPAIR TIMES

Position	Type	Repair Time (min.)
Sub150	Substation	120
B13-18	Manual Switch	60
B57-60	Line	90
L49	Critical Load	60

We have studied 3 cases in this scenario. In Case 1, depot 1 has one operation crew and depot 2 has one repair crew. In Case 2, each depot has one operation crew and one repair crew. In both Cases 1 and 2, we assume that operation crew can only operate manual switches, and the repair crew can only operate the manual switch right after repairing it. In Case 3, we use the same crew allocation as in Case 2. However, we assume each crew can perform both operation and repair tasks.

b) Cases for Scenario II

In scenario II, we compared the computation capabilities of the proposed synthetic model with existing methods. We modified and implemented an existing method introduced in [29] and tested both two methods. In scenario II, the black-start DG at node 451 is assumed to be unavailable, which means only substation 450 is utilized as power source to pick up loads, and all 16 switches are assumed to be remote-controlled switches. We randomly generated 10 damaged branches (lines and switches) to test both methods, and the repair time for each of the damages is set to 60 minutes. We repeated the test 10 times.

2) Numerical Results and Discussion

a) Scenario I

In case 1 in this scenario, both the substation 150 and the black-start DG451 are utilized as power sources for the restoration process. Fig. 6 shows the simplified system topology with only node cells and switches at the start time and end time of the restoration process. Fig. 7 depicts the detailed operation/repair/energization sequence for OA/RA/EA during the restoration.

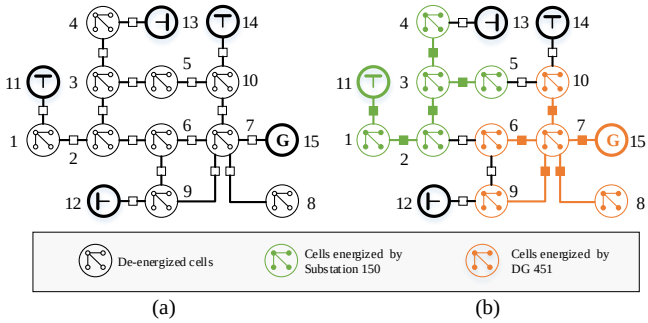

Fig. 6. Node cell energization status at the start (a) and end (b) times.

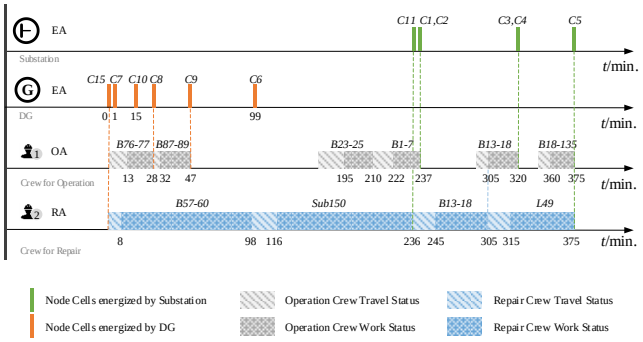

Fig. 7. Repair and restoration sequence for EA/OA/RA

In Case 1, as depicted in Fig.6-7, two sub-systems are formed after the restoration, of which the root nodes are substation 150 and DG 451, respectively. DG 451 energies node cells 6 – 10 by sequentially closing three remote switches and two manual switches. DG 451 cannot pick up more loads because of the power capacity limit. Substation 150 energies cells 1 – 5 by closing two remote switches and three manual switches. Damage line B57-60 is repaired at 98th minute right before remote-controlled switch B60-160 is closed at 99th minute so that node cell 6 can be picked-up. Substation 150 will be energized once it is repaired at the 236th minute. Damaged manual switch 13-18 is repaired at the 305th minute and then closed by the operation crew, thus saving time for repair crew to repair Load L49. All the loads are picked up by substation 150 and DG 451 until the last cell C5 was energized at the 375th minute. The restored load and unserved energy are depicted in Fig. 8, in which the restored load is 3,385 kW by 375th minute and the total amount of unserved energy is 9,178 kWh represented by the meshed area.

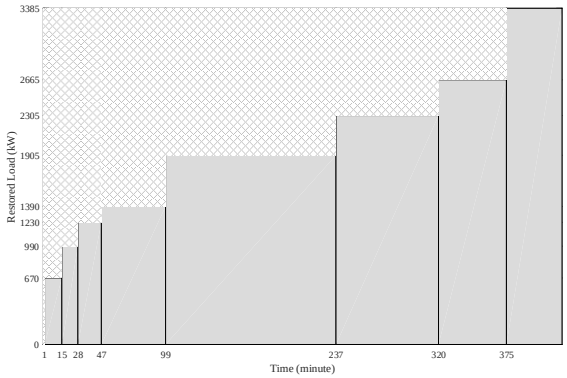

Fig. 8. Restored load and total amount of unserved energy.

The results of restoration completion time and unserved energy, crew routing and task completion time, as well as switching sequences and node cell pick-up sequences for Cases 1 – 3 are listed in TABLE VIII – X, respectively.

TABLE VIII. RESTORATION RESULTS FOR CASES 1 – 3

	Case		
	1	2	3
Completion Time (min.)	375	210	133
Unserved Energy (kWh)	9178	5618	4328
Computation Time (sec.)	8.6	3.4	3.3

TABLE IX. CREW ROUTING AND COMPLETION TIME FOR CASES 1 – 3

Case No.	Crew Routing	Completion Time (min.)
1	OA@D1: D1 → M76-77 → M87-89 → M23-25 → M1-7 → M13-18 → M18-135	375
	RA@D2: D2 → B57-60 → S150 → B13-18 → L49	375
2	OA@D1: D1 → M87-89 → M23-25 → M13-18	182
	OA@D2: D2 → M76-77 → M1-7 → M18-135	210
	RA@D1: D1 → S150 → L49	210
	RA@D2: D2 → B57-60 → M13-18	167
3	Crew1: D1 → S150	132
	Crew2: D1 → M87-89 → B13-18 → M18-135	133
	Crew3: D2 → B57-60 → M1-7	126
	Crew4: D2 → M76-77 → L49 → M23-25 → M54-94 → B151-300	161

D: Depot; M: Manually operated switch; B: damaged branches; S: Substation; L: Load.

TABLE X. SWITCHING SEQUENCE AND CELL PICK-UP TIMES FOR CASES 1 – 3

Case 1			Case 2			Case 3		
Time (min.)	SSEQ.	Cells	Time (min.)	SSEQ.	Cells	Time (min.)	SSEQ.	Cells
1	R450-451	7	1	R450-451	7	1	R450-451	7
15	R97-197	10	15	R97-197	10	2	R97-197	10
28	M76-77	8	25	M87-89	9	24	M87-89	9
47	M87-89	9	28	M76-77	8	28	M76-77	8
99	R60-160	6	99	R60-160	6	99	R60-160	6
210	M23-25		133	R150-149	1	114	M13-18	
				M1-7	2			
237	R150-149	1	156	M23-25		126	M1-7	
	M1-7	2						
320	M13-18	3,4	182	M13-18	3,4	128	M23-25	
375	M18-135	5	210	M18-135	5	133	R150-149 M18-135	1–5

SSEQ: Switching sequence; R: Remote-controlled switch; M: Manually-operated switch.

In Case 2, two repair crews go to the damage sites and two operation crews go to close manual switches. In Case 2, both the repair work and operation work are completed earlier than Case 1, thus the unserved energy is less than that of Case 1. It should be noted that, although adding more repair crews will accelerate the restoration process, improvements to the restoration time are also restricted by the crew's pre-stage and resource allocation decisions during the preventive response stage, which will be the focus of our future work. In Case 3, all the four crews are assumed to have no differences on working skills/expertise. The crew routing results in TABLE IX show that all the four crews complete repairing work and operating intact manual switches, and the restoration completion time and unserved energy is less than that in Case 2. It is also worth noticing that, the service restoration process often involves crews of different skills (e.g., tree trimming, manual switch operation, damages repair, resource deliver etc.). In the future work, we will extend the proposed synthetic model to consider more skills of crews.

b) Scenario II

The existing methods [25-29, 36] feature pre-determined time horizon, which is evenly divided into multiple time intervals. Decision variables and system state variables must be defined for each time interval. However, the length of time horizon is not required in the proposed routing-based synthetic model. In addition, the control actions are not limited to be defined at a fixed time interval but can be assigned accurate operation time. For simplicity, we refer the existing method [29, 36] as fixed-time step (FTS) model, and the proposed method as variable time step (VTS) model. It should be noted that, to make these two methods comparable on computation time, we didn't consider the pre-processing method of clustering damages to different depots as proposed in [29]. The comparison of objective and computation time results for these two methods are listed in TABLE XI.

TABLE XI. CASE RESULTS COMPARISON OF SCENARIO II

Case No.	Objective value / Best integer value (kWh)			Computation Time (sec.) / MIP gap		
	FTS	VTS	Objective Improved	FTS	VTS	Time saved
1	7409	7281	1.73%	833	39	95.3%
2	7161	6907	3.55%	1266	58	95.4%
3*	**9661**	**9302**	**3.72%**	**(21.8%)**	**2362**	**NA**
4	7021	6739	4.02%	1728	62	96.4%
5	6741	6638	1.53%	757	60	92.1%
6	5978	5957	0.35%	1368	142	89.6%
7	5448	5341	1.96%	2468	42	98.3%
8*	**8244**	**8092**	**1.84%**	**(4.63%)**	**822**	**NA**
9	7989	7281	8.86%	194	37	80.9%
10	8199	7882	3.87%	1824	552	69.7%

* For FTS results of case 3 and 8, CPLEX cannot converged within the given MIP gap tolerance after 3600 seconds (time limit), thus the objective value is the incumbent value with MIP gap listed in the corresponding lines.

TABLE XI shows that the proposed model achieved slightly better objective values but saved a large fraction of computation time compared to the FTS model. It is worth noticing that for Cases 3 and 8, the computation time of the FTS model exceeds the given time limit (i.e., 3600 seconds), and we listed the MIP gap values as references. Whereas the proposed VTS model can achieve the optimal value within the time limit.

B. Test on Large-scale Distribution Test Feeders

1) Test Feeder and Case Design

We have tested the proposed method on four large-scale distribution test feeders, i.e. the EPRI ckt5, ckt7, ckt24 [37] and IEEE 8500 node test feeder [35], as shown in Fig. 9. The size of these four test feeders are listed in TABLE XII. We used the reduction algorithm introduced in [38] to replace the laterals without switches with equivalent models while keeping the rest of system unchanged. The number of switches and node cells are listed in TABLE XIII. We used the switches that originally

come with EPRI Ckt5 and IEEE 8500 node test feeders (for simplicity we use IEEE8500 to represent below), of which we randomly chose 20 and 10 switches as manual switches. Since the switch information is not available in the original data of Ckt7 and Ckt24, we added 36 and 70 switches, and randomly chose 10 and 20 out of them as manual switches. We set four depots for each test feeder, and the number of crews in each depot was set to be 5, 4, 5 and 4 for Ckt5, Ckt7, Ckt24 and IEEE8500, respectively. Every crew is assumed to have the skills of performing both operation and repair tasks. Besides, we generated 20 branch damages, and the repair time of these damages is generated randomly between 60 – 3600 minutes. The MIP gap tolerance is set to be 5% and time limit is set to be 3600 seconds.

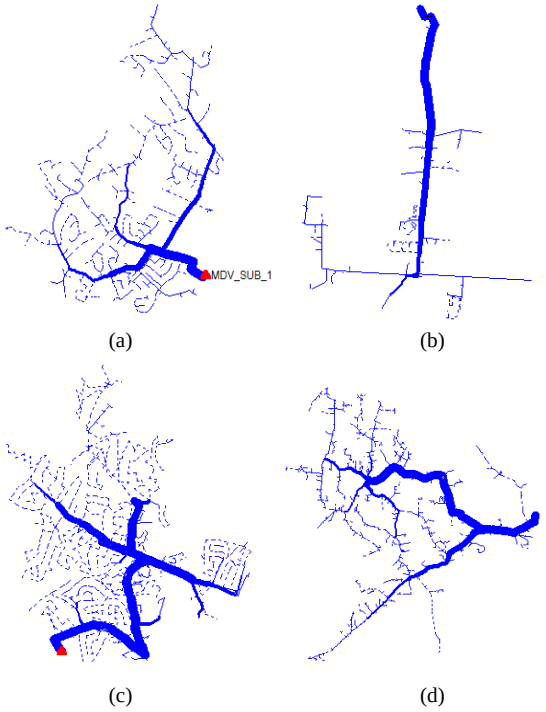

Fig. 9. Large-scale distribution test feeders: (a) EPRI Ckt5; (b) EPRI Ckt7; (c) EPRI Ckt24; (d) IEEE 8500 node test feeder.

TABLE XII. SYSTEM SUMMARY OF CKT5, CKT7, CKT24 AND IEEE 8500

Feeder	Number of Buses		Number of Branches		Total Loads (kW)*
	Before Reduction	After Reduction	Before Reduction	After Reduction	
Ckt5	2918	300	2927	299	7133
Ckt7	1255	91	1254	90	5601
Ckt24	2167	294	2166	293	11253
IEEE8500	3698	719	3702	723	10773

* The total loads exclude the loads in the substation.

TABLE XIII. PROBLEM SETUP OF CKT5, CKT7, CKT24 AND IEEE8500

Feeder	Switches	Node Cells	Manual Switches	Depots	Crews	Damages
Ckt5	70	71	20	4	20	20
Ckt7	36	37	10	4	16	20
Ckt24	70	71	20	4	20	20
IEEE8500	43	39	10	4	16	20

2) Numerical Results and Discussion

The restoration results for these four large-scale feeders are listed in TABLE XIV. The load restoration processes are depicted in Fig. 10 (a – d).

TABLE XIV. RESTORATION RESULTS FOR LARGE-SCALE FEEDERS

Feeder	Ckt5	Ckt7	Ckt24	IEEE8500
Completion Time (min.)	376	374	370	409
Unserved Energy (kWh)	34827	30590	48584	61853
Computation Time (sec.)	70.4	11.6	153.8	124.1

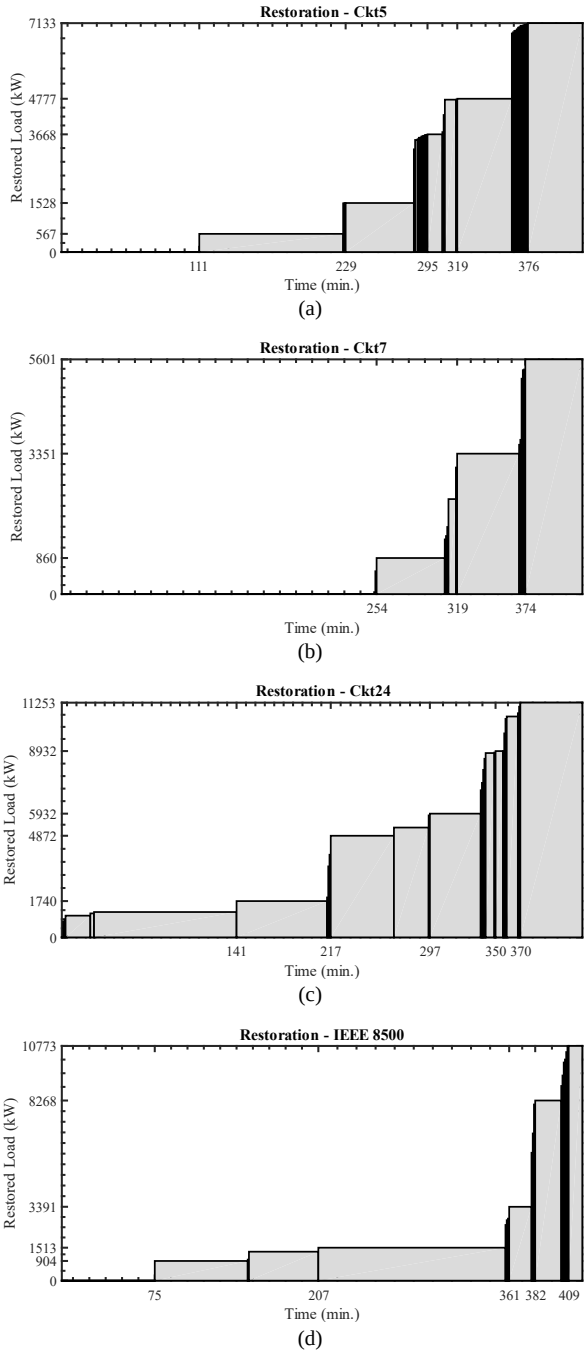

Fig. 10. Restored load of (a) EPRI Ckt5; (b) EPRI Ckt7; (c) EPRI Ckt34; (d) IEEE 8500 node test feeder.

The results in TABLE XIV show that the proposed model is effective in solving the synthetic DSR and crew dispatch problems on large-scale test feeders, and the computation time is acceptable at the given the tolerance. Fig. 10 presented a sequence of coordinated operations of remote-controlled switches, manual switches and crew repair work. The figures show that the solution of the proposed model can supply utility operators more accurate restoration and dispatch solutions.

VI. Conclusion

A synthetic MILP model for distribution system restoration and crew dispatch was proposed to coordinate multiple DSR tasks including switch operation, crew dispatch, and component repair. The concepts of "energization agent" and "energization path" were introduced and used to formulate the DSR problem as a routing problem. Skill sets for different types of crews were also considered in the integrated model based on the universal routing model. Numerical results showed that the proposed model can generate an optimal synthetic restoration solution, which considers the switching sequence of remote-controlled and manually operated switches, optimal routing sequence of operation and repair crews, as well as load energization sequence. The comparative studies exhibited the advantages of the proposed model on computation time and objective values, compared to that of the existing FTS models. Case study results on several large-scale test feeders also showed the potential of applying the proposed model in the large-scale distribution systems. Future work will integrate this model with preventive crew pre-positioning and resource allocation decisions for better strategic resilience enhancement.

VII. References

[1] Y. Wang, C. Chen, J. Wang, and R. Baldick, "Research on Resilience of Power Systems Under Natural Disasters-A Review," *IEEE Transactions on Power Systems,* vol. 31, no. 2, pp. 1604-1613, 2016.

[2] National Academies of Sciences, Engineering and Medicine, *Enhancing the Resilience of the Nation's Electricity System*, Washington, DC: The National Academies Press, 2017.

[3] US. Department of Energy, "Hurricanes Nate, Maria, Irma, and Harvey Situation Reports", Oct. 13, 2017. [Online]. Available: https://www.energy.gov/oe/downloads/hurricanes-nate-maria-irma-and-harvey-situation-reports.

[4] R. Perez-Guerrero, G. T. Heydt, N. J. Jack, B. K. Keel, and A. R. Castelhano, "Optimal Restoration of Distribution Systems Using Dynamic Programming," *IEEE Transactions on Power Delivery,* vol. 23, no. 3, pp. 1589-1596, 2008.

[5] I. Watanabe and M. Nodu, "A genetic algorithm for optimizing switching sequence of service restoration in distribution systems," *Proceedings of the 2004 Congress on Evolutionary Computation*, Portland, OR, USA, 2004, pp. 1683-1690 Vol.2.

[6] J. Li, X. Y. Ma, C. C. Liu, and K. P. Schneider, "Distribution System Restoration With Microgrids Using Spanning Tree Search," *IEEE Transactions on Power Systems,* vol. 29, no. 6, pp. 3021-3029, 2014.

[7] P. M. S. Carvalho, F. J. D. Carvalho and L. A. F. M. Ferreira, "Dynamic Restoration of Large-Scale Distribution Network Contingencies: Crew Dispatch Assessment," *2007 IEEE Lausanne Power Tech*, Lausanne, 2007, pp. 1453-1457.

[8] D. P. Bernardon, M. Sperandio, V. J. Garcia, L. N. Canha, A. d. R. Abaide, and E. F. B. Daza, "AHP Decision-Making Algorithm to Allocate Remotely Controlled Switches in Distribution Networks," *IEEE Transactions on Power Delivery,* vol. 26, no. 3, pp. 1884-1892, 2011.

[9] A. Zidan, M. Khairalla, A. M. Abdrabou, T. Khalifa, K. Shaban, A. Abdrabou, R. E. Shatshat, and A. M. Gaouda, "Fault Detection, Isolation, and Service Restoration in Distribution Systems: State-of-the-Art and Future Trends," *IEEE Transactions on Smart Grid,* vol. 8, no. 5, pp. 2170-2185, 2017.

[10] M. H. M. Camillo *et al*., "Determination of switching sequence of Service Restoration in Distribution Systems: Application and analysis on a real and large-scale radial system," *2016 IEEE/PES Transmission and Distribution Conference and Exposition (T&D)*, Dallas, TX, 2016, pp. 1-5.

[11] C. Chen, J. Wang, and D. Ton, "Modernizing Distribution System Restoration to Achieve Grid Resiliency Against Extreme Weather Events: An Integrated Solution," *Proceedings of the IEEE,* vol. 105, no. 7, pp. 1267-1288, 2017.

[12] Q. Chen, X. Zhao, and D. Gan, "Active-reactive scheduling of active distribution system considering interactive load and battery storage," *Protection and Control of Modern Power Systems,* vol. 2, no. 1, pp. 29, 2017/08/07, 2017.

[13] P. M. d. Quevedo, J. Contreras, M. J. Rider, and J. Allahdadian, "Contingency Assessment and Network Reconfiguration in Distribution Grids Including Wind Power and Energy Storage," *IEEE Transactions on Sustainable Energy,* vol. 6, no. 4, pp. 1524-1533, 2015.

[14] X. Chen, W. Wu, and B. Zhang, "Robust Restoration Method for Active Distribution Networks," *IEEE Transactions on Power Systems,* vol. 31, no. 5, pp. 4005-4015, 2016.

[15] A. Kwasinski, V. Krishnamurthy, J. Song, and R. Sharma, "Availability Evaluation of Micro-Grids for Resistant Power Supply During Natural Disasters," *IEEE Transactions on Smart Grid,* vol. 3, no. 4, pp. 2007-2018, 2012.

[16] Y. Xu, C. C. Liu, K. Schneider, F. Tuffner, and D. Ton, "Microgrids for Service Restoration to Critical Load in a Resilient Distribution System," *IEEE Transactions on Smart Grid,* vol. PP, no. 99, pp. 1-1, 2016.

[17] H. Gao, Y. Chen, Y. Xu, and C. C. Liu, "Resilience-Oriented Critical Load Restoration Using Microgrids in Distribution Systems," *IEEE Transactions on Smart Grid,* vol. 7, no. 6, pp. 2837-2848, 2016.

[18] C. Chen, J. Wang, F. Qiu, and D. Zhao, "Resilient Distribution System by Microgrids Formation After Natural Disasters," *IEEE Transactions on Smart Grid,* vol. 7, no. 2, pp. 958-966, 2016.

[19] Y. Xu, C. Liu, K. P. Schneider, and D. T. Ton, "Placement of Remote-Controlled Switches to Enhance Distribution System Restoration Capability," *IEEE Transactions on Power Systems,* vol. 31, no. 2, pp. 1139-1150, 2016.

[20] S. Lei, J. Wang, and Y. Hou, "Remote-Controlled Switch Allocation Enabling Prompt Restoration of Distribution Systems," *IEEE Transactions on Power Systems,* vol. 33, no. 3, pp. 3129-3142, 2018.

[21] P. L. Cavalcante, J. C. López, J. F. Franco, M. J. Rider, A. V. Garcia, M. R. R. Malveira, L. L. Martins, and L. C. M. Direito, "Centralized Self-Healing Scheme for Electrical Distribution Systems," *IEEE Transactions on Smart Grid,* vol. 7, no. 1, pp. 145-155, 2016.

[22] Z. Wang, and J. Wang, "Self-Healing Resilient Distribution Systems Based on Sectionalization Into Microgrids," *IEEE Transactions on Power Systems,* vol. 30, no. 6, pp. 3139-3149, 2015.

[23] B. Chen, C. Chen, J. Wang, and K. L. Butler-Purry, "Multi-Time Step Service Restoration for Advanced Distribution Systems and Microgrids," *IEEE Transactions on Smart Grid,* vol. 9, no. 6, pp. 6793-6805, 2018.

[24] B. Chen, C. Chen, J. Wang, and K. L. Butler-Purry, "Sequential Service Restoration for Unbalanced Distribution Systems and Microgrids," *IEEE Transactions on Power Systems,* vol. 33, no. 2, pp. 1507-1520, 2018.

[25] A. Arab, A. Khodaei, Z. Han, and S. K. Khator, "Proactive Recovery of Electric Power Assets for Resiliency Enhancement," *IEEE Access,* vol. 3, pp. 99-109, 2015.

[26] P. Van Hentenryck, and C. Coffrin, "Transmission system repair and restoration," *Mathematical Programming,* vol. 151, no. 1, pp. 347-373, 2015/06/01, 2015.

[27] C. Coffrin and P. Van Hentenryck, "Transmission System Restoration: Co-optimization of repairs, load pickups, and generation dispatch," *2014 Power Systems Computation Conference*, Wroclaw, 2014, pp. 1-8.

[28] P. Van Hentenryck, C. Coffrin, and R. Bent, "Vehicle routing for the last mile of power system restoration," *Proceedings of the 17th Power Systems Computation Conference (PSCC'll)*, Stockholm, Sweden, 2011.

[29] A. Arif, Z. Wang, J. Wang, and C. Chen, "Power Distribution System Outage Management with Co-Optimization of Repairs, Reconfiguration, and DG Dispatch," *IEEE Transactions on Smart Grid,* vol. PP, no. 99, pp. 1-1, 2017.

[30] A. Arif, S. Ma, Z. Wang, J. Wang, S. M. Ryan and C. Chen, "Optimizing Service Restoration in Distribution Systems With Uncertain Repair Time and Demand," in *IEEE Transactions on Power Systems*, vol. 33, no. 6, pp. 6828-6838, Nov. 2018.
[31] B. Chen, Z. Ye, C. Chen, and J. Wang, "Toward a MILP Modeling Framework for Distribution System Restoration," *IEEE Transactions on Power Systems*, accepted.
[32] W. H. Kersting, *Distribution System Modeling and Analysis, Third Edition*: CRC Press, 2012.
[33] G. Huang, J. Wang, C. Chen, J. Qi, and C. Guo, "Integration of Preventive and Emergency Responses for Power Grid Resilience Enhancement," *IEEE Transactions on Power Systems*, vol. 32, no. 6, pp. 4451-4463, 2017.
[34] K. P. Schneider, B. A. Mather, B. C. Pal, C. Ten, G. J. Shirek, H. Zhu, J. C. Fuller, J. L. R. Pereira, L. F. Ochoa, L. R. d. Araujo, R. C. Dugan, S. Matthias, S. Paudyal, T. E. McDermott, and W. Kersting, "Analytic Considerations and Design Basis for the IEEE Distribution Test Feeders," *IEEE Transactions on Power Systems*, vol. 33, no. 3, pp. 3181-3188, 2018.
[35] IEEE PES AMPS DSAS Test Feeder Working Group, "IEEE test feeders" [Online]. Available: http://sites.ieee.org/pes-testfeeders/resources/.
[36] A. Arif, S. Ma, Z. Wang, J. Wang, S. M. Ryan, and C. Chen, "Optimizing Service Restoration in Distribution Systems With Uncertain Repair Time and Demand," *IEEE Transactions on Power Systems*, vol. 33, no. 6, pp. 6828-6838, 2018.
[37] Electric Power Research Institute, "EPRI test circuits," [Online]. Available: http://svn.code.sf.net/p/electricdss/code/trunk/Distrib/EPRITestCircuits/.
[38] Z. K. Pecenak, V. R. Disfani, M. J. Reno, and J. Kleissl, "Multiphase Distribution Feeder Reduction," *IEEE Transactions on Power Systems*, vol. 33, no. 2, pp. 1320-1328, 2018.

Bo Chen (M'17) received the Ph.D. degree in electrical engineering from Texas A&M University, College Station, USA, in 2017. He received the B.S. and M.S. degrees from North China Electric Power University, Baoding, China. In 2016, he worked as a research aide at the Argonne National Laboratory, IL, USA. Currently, he is a postdoctoral researcher at the Energy Systems Division, Argonne National Laboratory, IL, USA. His research interests include modeling, control, and optimization of power systems, cybersecurity, and cyber-physical systems.

Zhigang Ye (S'17) received the B.S. degrees from Xi'an Jiaotong University, Xi'an, China, in 2013, and he is currently pursuing his Ph.D. degree in the same university. He was also a visiting student at Texas A&M University, College Station, USA, during Oct. 2016 – Jul. 2017, and a visiting student at the Energy System Division, Argonne National Laboratory, IL, USA during Aug. 2017 – Oct. 2018. His research interests include modeling of power system reliability and resilience, and algorithms for bilevel mixed-integer programming.

Chen Chen (M'13) received the B.S. and M.S. degrees from Xi'an Jiaotong University, Xi'an, China, in 2006 and 2009, respectively, and the Ph.D. degree in electrical engineering from Lehigh University, Bethlehem, PA, USA, in 2013. During 2013-2015, he worked as a Postdoctoral Researcher at the Energy Systems Division, Argonne National Laboratory, Argonne, IL, USA. Dr. Chen is currently an Energy Systems Scientist with the Energy Systems Division at Argonne National Laboratory. His primary research is in optimization, communications and signal processing for smart electric power systems, power system resilience, and cyber-physical system modeling for smart grids. He is an editor of IEEE Transactions on Smart Grid and IEEE Power Engineering Letters.

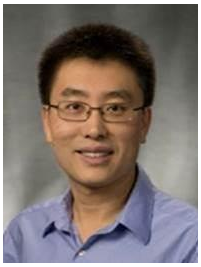

Jianhui Wang (M'07-SM'12) received the Ph.D. degree in electrical engineering from Illinois Institute of Technology, Chicago, Illinois, USA, in 2007. Presently, he is an Associate Professor with the Department of Electrical Engineering at Southern Methodist University, Dallas, Texas, USA. Prior to joining SMU, Dr. Wang had an eleven-year stint at Argonne National Laboratory with the last appointment as Section Lead – Advanced Grid Modeling. Dr. Wang is the secretary of the IEEE Power & Energy Society (PES) Power System Operations, Planning & Economics Committee. He has held visiting positions in Europe, Australia and Hong Kong including a VELUX Visiting Professorship at the Technical University of Denmark (DTU). Dr. Wang is the Editor-in-Chief of the IEEE Transactions on Smart Grid and an IEEE PES Distinguished Lecturer. He is also a Clarivate Analytics highly cited researcher for 2018.

Tao Ding (S'13 – M'15) received the B.S.E.E. and M.S.E.E. degrees from Southeast University, Nanjing, China, in 2009 and 2012, respectively, and the Ph.D. degree from Tsinghua University, Beijing, China, in 2015. During 2013 and 2014, he was a Visiting Scholar in the Department of Electrical Engineering and Computer Science, University of Tennessee, Knoxville, TN, USA. He is currently an Associate Professor in the State Key Laboratory of Electrical Insulation and Power Equipment, the School of Electrical Engineering, Xi'an Jiaotong University. His current research interests include electricity markets, power system economics and optimization methods, and power system planning and reliability evaluation. He has published more than 60 technical papers and authored by "Springer Theses" recognizing outstanding Ph.D. research around the world and across the physical sciences – Power System Operation with Large Scale Stochastic Wind Power Integration. He received the excellent master and doctoral dissertation from Southeast University and Tsinghua University, respectively, and Outstanding Graduate Award of Beijing City. Dr. Ding is an Associate Editor of CSEE Journal of Power and Energy Systems.

Zhaohong Bie (M'98–SM'12) received the B.S. and M.S. degrees in electric power from Shandong University, Jinan, China, and the Ph.D. degree from Xi'an Jiaotong University, Xi'an, China, in 1992, 1994, and 1998, respectively. Currently, she is a professor with the State Key Laboratory of Electrical Insulation and Power Equipment and the School of Electrical Engineering, Xi'an Jiaotong University. Her research interests include power system planning and reliability evaluation, as well as the integration of the renewable energy.